Article citation info:
Kustosz J, Magnucki K, Goliwąs D. Strength of a bent sandwich beam with clamped ends. Rail Vehicles/Pojazdy Szynowe. 2023;1-2:3-7. https://doi.org/10.53502/RAIL-161868

Rail Vehicles/Pojazdy Szynowe

www.railvehicles.eu

Strength of a bent sandwich beam with clamped ends

Joanna **Kustosz** [a, *], Krzysztof **Magnucki** [a], Damian **Goliwąs** [a]

[a] *Łukasiewicz Research Network – Poznan Institute of Technology, Poznan, Poland*

ARTICLE INFO

Received: 5 December 2022
Revised: 27 February 2023
Accepted: 4 March 2023
Available online: 5 March 2023

KEYWORDS

Deflection
Classical sandwich beam
Supports – clamped ends
Shear effect
Stresses

The subject of the work is a symmetrical sandwich beam with clamped ends under uniformly distributed load. The system of two equilibrium equations, formulated taking into account the literature, was solved analytically. The function of the shear effect and the maximum deflection of the beam were determined. The stress state at the clamped end of the beam is described in detail. The significant influence of the shear effect on the normal stresses in the outer layers of the beam near the clamped end was indicated. Exemplary calculations were made for the adopted family of beams. Moreover, the numerical FEM model of the beam was developed and calculations were made for this adopted family of beams. A comparative analysis of the obtained results was carried out.

1. Introduction

The sandwich structures are intensively improved in 21st century and used in different engineering constructions. Icardi [4] presented the zig-zag theory for the analysis of laminated and sandwich beams and pointed out the advantages of using higher-order approximations of displacements in sublaminates. Carrera and Brischetto [2] presented a review of the problems on bending and vibration of sandwich panels and various theories: classical, higher order, zig-zag, layered and mixed. Birman and Kardomateas [1] reviewed the theoretical basis and problems in the design of sandwich structures. Moreover, the author indicated their possible applications in the aerospace, civil and marine engineering. Hao et al. [3] presented a new model of a multilayer beam under three-point bending with clamped ends and proposed a theoretical prediction of its large deflection. Kozak [5] described the steel sandwich panels and their applications in ship structures. Magnucki [7] pointed out the similarity of the analytical modelling of the sandwich beam and the homogenous I-beam. Sayyad and Ghugal [10] presented the review of the 250 selected papers on the modelling functionally graded sandwich beam and suggested possible areas for further research. Magnucki et al. [8] studied analytically, numerically and experimentally four-point bending of the simply supported sandwich plate-strip. Magnucki et al. [9] developed three analytical models of the simply supported sandwich beam and investigated analytically end numerically its bending, buckling and free flexural vibration. Kustosz et al. [6] presented the bending problem of the stepped sandwich beam with clamped ends subjected to uniformly distributed load. The detailed calculations were carried out analytically and numerically FEM for exemplary beams.

The subject of the paper is a classical sandwich beam of length L with clamped ends subjected to the uniformly distributed load of intensity q (Fig. 1).

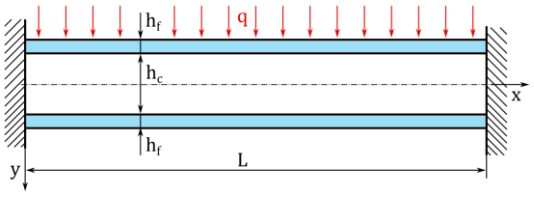

Fig. 1. Scheme of the sandwich beam

The cross section of the beam is a rectangle with depth h and width b. The thicknesses of the faces are h_f, whereas of the core is h_c, therefore $h = 2h_f + h_c$.

* Corresponding author: joanna.kustosz@pit.lukasiewicz.gov.pl (J. Kustosz)

2. Analytical studies of the beam bending

2.1. Analytical model of the beam

Taking into account the papers [7–9], the plane cross section of the sandwich beam with consideration of the "broken line" theory is deformed after its bending as shown in Fig. 2.

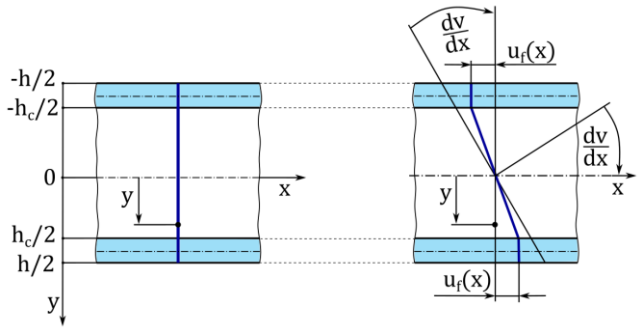

Fig. 2. Scheme of the beam cross-section deformation

The longitudinal displacements based on the above scheme (Fig. 2) are as follows:

- the upper face $-1/2 \le \eta \le -\chi_c/2$

$$u^{(uf)}(x,\eta) = -h\left[\eta\frac{dv}{dx} + \psi_f(x)\right] \tag{1}$$

- the core $-\chi_c/2 \le \eta \le \chi_c/2$

$$u^{(c)}(x,\eta) = -h\eta\left[\frac{dv}{dx} - \frac{2}{\chi_c}\psi_f(x)\right] \tag{2}$$

- the lower face $\chi_c/2 \le \eta \le 1/2$

$$u^{(lf)}(x,\eta) = -h\left[\eta\frac{dv}{dx} - \psi_f(x)\right] \tag{3}$$

where: $\eta = y/h$ – dimensionless coordinate, $v(x)$ – deflection, $\chi_c = h_c/h$ – dimensionless thickness of the core, $\psi_f(x) = u_f(x)/h$ – dimensionless longitudinal displacement – shear effect function.

Consequently, the strains and stresses in successive layers are in the form:

- the upper face $-1/2 \le \eta \le -\chi_c/2$

$$\varepsilon_x^{(uf)}(x,\eta) = \frac{\partial u}{\partial x} = -h\left[\eta\frac{d^2v}{dx^2} + \frac{d\psi_f}{dx}\right] \tag{4}$$

$$\gamma_{xy}^{(uf)}(x,\eta) = \frac{\partial u}{\partial y} + \frac{dv(x)}{dx} = 0 \tag{5}$$

$$\sigma_x^{(uf)}(x,\eta) = E_f\varepsilon_x^{(uf)}(x,\eta) \tag{6}$$

- the core $-\chi_c/2 \le \eta \le \chi_c/2$

$$\varepsilon_x^{(c)}(x,\eta) = \frac{\partial u}{\partial x} = -h\eta\left[\frac{d^2v}{dx^2} - \frac{2}{\chi_c}\frac{d\psi_f}{dx}\right] \tag{7}$$

$$\gamma_{xy}^{(c)}(x,\eta) = \frac{\partial u}{\partial y} + \frac{dv(x)}{dx} = \frac{2}{\chi_c}\psi_f(x) \tag{8}$$

$$\sigma_x^{(c)}(x,\eta) = E_c\varepsilon_x^{(c)}(x,\eta) \tag{9}$$

$$\tau_{xy}^{(c)}(x,\eta) = \frac{E_c}{2(1+\nu_c)}\gamma_{xy}^{(c)}(x,\eta) \tag{10}$$

- the lower face $\chi_c/2 \le \eta \le 1/2$

$$\varepsilon_x^{(lf)}(x,\eta) = \frac{\partial u}{\partial x} = -h\left[\eta\frac{d^2v}{dx^2} - \frac{d\psi_f}{dx}\right] \tag{11}$$

$$\gamma_{xy}^{(lf)}(x,\eta) = \frac{\partial u}{\partial y} + \frac{dv(x)}{dx} = 0 \tag{12}$$

$$\sigma_x^{(lf)}(x,\eta) = E_f\varepsilon_x^{(uf)}(x,\eta) \tag{13}$$

where: E_f, E_c – Young's modules of faces and the core, ν_c – Poisson ratio of the core.

Taking into account the principle of the maximum potential energy $\delta(U_\varepsilon - W) = 0$, the system of two differential equations of equilibrium of this beam is in the following form:

$$C_{vv}\frac{d^2v}{dx^2} - C_{v\psi}\frac{d\psi_f}{dx} = -12\frac{M_b(x)}{E_f b h^3} \tag{14}$$

$$C_{v\psi}\frac{d^3v}{dx^3} - C_{\psi\psi}\frac{d^2\psi_f}{dx^2} + C_\psi\frac{\psi_f(x)}{h^2} = 0 \tag{15}$$

where: dimensionless coefficients
$C_{vv} = 1 - (1 - e_c)\chi_c^3$, $C_{v\psi} = 3 - (3 - 2e_c)\chi_c^2$
$C_{\psi\psi} = 4[3 - (3 - e_c)\chi_c]$, $C_\psi = \frac{24}{1+\nu_c}\frac{e_c}{\chi_c}$, $e_c = \frac{E_c}{E_f}$
and the bending moment

$$M_b(x) = \frac{1}{2}(xL - x^2)q - M_c \tag{16}$$

where M_c – the unknown clamped-ends moment.

This moment (16) is formulated based on the Fig. 3. The vertical reaction $R = qL/2$.

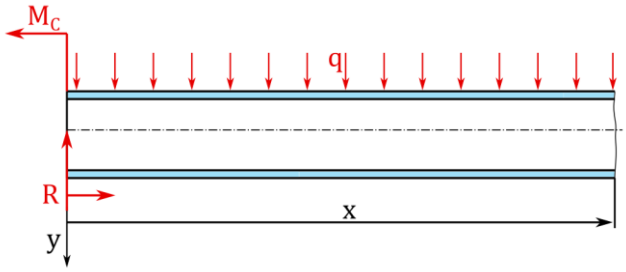

Fig. 3. Scheme of the beam end with the load and reactions

2.2. Analytical research of the stress state in the beam

The system of two differential equations (14) and (15) with consideration of the bending moment (16) after simple transformation, is reduced to one differential equation

$$\frac{d^2\psi_f}{d\xi^2} - (\alpha\lambda)^2\psi_f(\xi) = -6\frac{(1-2\xi)C_{v\psi}}{C_{vv}C_{\psi\psi} - C_{v\psi}^2}\frac{q\lambda^3}{E_f b} \tag{17}$$

where: $\xi = x/L$ – the dimensionless coordinate, $\lambda = L/h$ – relative length of the beam, and $\alpha = \sqrt{\frac{C_{vv}C_\psi}{C_{vv}C_{\psi\psi} - C_{v\psi}^2}}$ – the dimensionless coefficient.

The solution of this equation is the shear effect function in the form

$$\Psi_f(\xi) = C_1 \sinh(\alpha\lambda\xi) + C_2 \cosh(\alpha\lambda\xi) + \\ +6(1-2\xi)\frac{C_{v\psi}}{C_{vv}C_\psi}\lambda\frac{q}{E_f b} \tag{18}$$

where: C_1, C_2 – integration constants.

Taking into account the following two conditions: $\psi_f(0) = 0$ – clamped end, and $\psi_f(1/2) = 0$ – symmetry plane of the beam, these constants are determined as follows $C_1 = -\frac{C_2}{\tanh(\alpha\lambda/2)}$, $C_2 = -6\frac{C_{v\psi}}{C_{vv}C_\psi}\lambda\frac{q}{E_f b}$.

Thus, the function (18) is in the following form

$$\Psi_f(\xi) = \tilde{\psi}_f(\xi)\frac{q}{E_f b} \tag{19}$$

where

$$\tilde{\psi}_f(\xi) = 6\left\{1 - 2\xi - \frac{\sinh[(1-2\xi)\alpha\lambda/2]}{\sinh(\alpha\lambda/2)}\right\}\frac{C_{v\psi}}{C_{vv}C_\psi}\lambda \tag{20}$$

The equation (14) with consideration of the expression (16), and in the dimensionless coordinate ξ, after first integration is as follows

$$C_{vv}\frac{d\bar{v}}{d\xi} = C_3 + C_{v\psi}\psi_f(\xi) - \\ -6\left(\frac{1}{2}\xi^2 - \frac{1}{3}\xi^3 - 2\bar{M}_c\xi\right)\lambda^3\frac{q}{E_f b} \tag{21}$$

where: $\bar{v}(\xi) = \frac{v(\xi)}{L}$ – the relative deflection, C_3 – the integration constant, $\bar{M}_c = \frac{M_c}{qL^2}$ – the dimensionless clamped-ends moment.

Taking into account two conditions: $\frac{d\bar{v}}{d\xi}|_0 = 0$ and $\psi_f(0) = 0$ one obtains the integration constant $C_3 = 0$, and based on conditions: $\frac{d\bar{v}}{d\xi}|_{1/2} = 0$ and $\psi_f\left(\frac{1}{2}\right) = 0$ one obtains the dimensionless moment $\bar{M}_c = \frac{1}{12}$.

Therefore, the equation (21) is in the form

$$C_{vv}\frac{d\bar{v}}{d\xi} = C_{v\psi}\psi_f(\xi) - (3\xi^2 - 2\xi^3 - \xi)\lambda^3\frac{q}{E_f b} \tag{22}$$

This equation after integration is as follows

$$C_{vv}\bar{v}(\xi) = \{C_4 + 6f_1(\xi)\frac{C_{v\psi}^2}{C_{vv}C_\psi}\lambda - \\ -\left(\xi^3 - \frac{1}{2}\xi^4 - \frac{1}{2}\xi^2\right)\lambda^3\}\frac{q}{E_f b} \tag{23}$$

where $f_1(\xi) = \xi - \xi^2 + \frac{\cosh[(1-2\xi)\alpha\lambda/2]}{\alpha\lambda\sinh(\alpha\lambda/2)}$ – the function, and C_4 – the integration constant.

Taking into account the condition $\bar{v}(0) = 0$, the integration constant was determined in the form

$$C_4 = -\frac{6}{\alpha\lambda\tanh(\alpha\lambda/2)}\frac{C_{v\psi}^2}{C_{vv}C_\psi}$$

Thus, the relative maximum deflection of this beam is as follows

$$\bar{v}_{max} = \bar{v}\left(\frac{1}{2}\right) = \tilde{v}_{max}\frac{q}{E_f b} \tag{24}$$

where the dimensionless maximum deflection

$$\tilde{v}_{max} = \left(1 + C_{se}^{(v)}\right)\frac{\lambda^3}{32C_{vv}} \tag{25}$$

and the shear effect coefficient of the bending

$$C_{se}^{(v)} = 48\left[1 - 4\frac{\cosh(\alpha\lambda/2)-1}{\alpha\lambda\sinh(\alpha\lambda/2)}\right]\frac{C_{v\psi}^2}{C_{vv}C_\psi}\frac{1}{\lambda^2} \tag{26}$$

The normal stresses (6) in the upper face with consideration of the expressions (19) and (22), after simply transformation, is as follows

$$\sigma_x^{(uf)}(\xi,\eta) = \left\{\left(1 + \eta\frac{C_{v\psi}}{C_{vv}}\right)f_2(\xi)\frac{C_{v\psi}}{C_\psi} + \\ +\eta\left(\xi - \xi^2 - \frac{1}{6}\right)\lambda^2\right\}\frac{1}{C_{vv}}\frac{q}{b} \tag{27}$$

where $f_2(\xi) = 2 - \alpha\lambda\frac{\cosh[(1-2\xi)\alpha\lambda/2]}{\sinh(\alpha\lambda/2)}$ – the function.

Therefore, the maximum normal stresses for the clamped end ($\xi = 0$) of the beam, and in the upper surface of its upper layer ($\eta = -1/2$), is as follows

$$\sigma_{x,max}^{(uf)} = \sigma_x^{(uf)}\left(0, -\frac{1}{2}\right) = \frac{1}{2}\left(1 + C_{se}^{(\sigma)}\right)\frac{\lambda^2}{C_{vv}}\frac{q}{b} \tag{28}$$

where the shear effect coefficient of the normal stress

$$C_{se}^{(\sigma)} = 12\left(\frac{C_{v\psi}}{C_{vv}} - 2\right)\left[\frac{\alpha\lambda}{2\tanh(\alpha\lambda/2)} - 1\right]\frac{C_{v\psi}}{C_\psi}\frac{1}{\lambda^2} \tag{29}$$

The detailed calculations are carried out for the exemplary sandwich beams with the following data: $\lambda = 20$, $\chi_c = 17/20$, $\nu_c = 0.3$, $e_c = 1/20, 1/35, 1/50$.

The shape of the shear effect function (20) is shown in the Fig. 4.

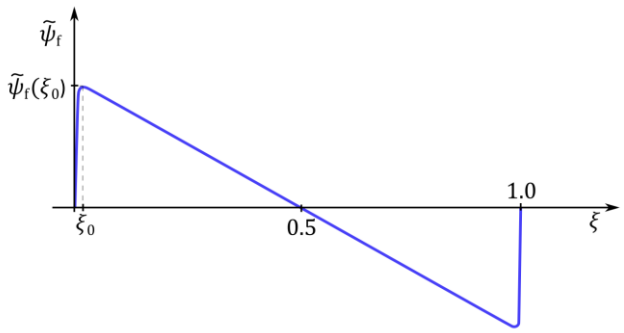

Fig. 4. The graph of the shear effect function (20)

The detailed calculation of the maximum values of the shear effect function (20) and the dimensionless coefficients (25) and (26) of the maximum deflections are specified in Table 1.

Table 1. The selected results – analytical calculations

e_c	1/20	1/35	1/50
ξ_0	0.170	0.0204	0.0231
$\tilde{\psi}_f(\xi_0)$	230.2	398.1	564.0
$C_{se}^{(v)}$	0.2142	0.3597	0.5045
$\tilde{v}_{max}$	728.66	842.60	944.65

Moreover, the values of the maximum normal stresses (28), with consideration of the value q/b = 1/10 MPa, are specified in the Table 2.

Table 2. The maximum normal stresses – analytical calculations

e_c	1/20	1/35	1/50
$C_{se}^{(\sigma)}$	0.6272	0.8091	0.9575
$\sigma_{x,max}^{(uf)}$ [MPa]	78.12	89.69	98.33

Analyzing the values of shear coefficients $C_{se}^{(v)}$ (Table 1) and $C_{se}^{(\sigma)}$ (Table 2) may be easily noticed that their values are large, therefore the share of the shear effect in the maximum deflection of the beam, and especially in normal stresses at the clamped end of the beam is significant.

3. Numerical FEM studies of the bending beam

3.1. Numerical FEM model of the beam

The numerical model of the tested sandwich beam was developed in the ABAQUS 6.12 system with the use of the same data as in analytical research. The model represents only half of the beam due to its symmetry. The mesh consists of 19551 hexahedral quadratic finite elements (Fig. 5).

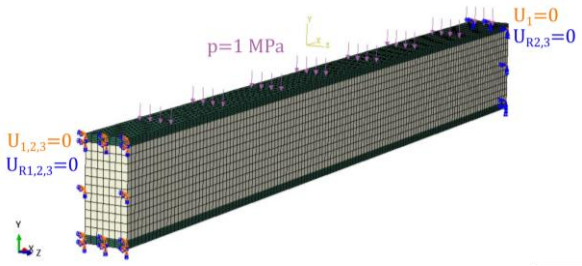

Fig. 5. The FEM numerical model of the example beam

3.2. Numerical FEM research of the beam

The results of numerical research of the maximal deflection of the beam are presented in Table 3. Moreover, the percentage differences between analytical and numerical value of the maximal deflection of the beam were obtained according to the formula $\Delta = \left(\left|\tilde{v}_{max}^{(AN)} - \tilde{v}_{max}^{(FEM)}\right| / \tilde{v}_{max}^{(AN)}\right) \cdot 100\%$.

Table 3. The maximal deflection results

e_c	1/20	1/35	1/50
$\tilde{v}_{max}^{(AN)}$	728.66	842.60	944.65
$\tilde{v}_{max}^{(FEM)}$	728.10	842.76	945.54
Δ	0.077	0.019	0.094

Similarly, the results of the maximum normal stresses at the clamped end of this sandwich beam are presented in Table 4.

Table 4. The maximum normal stresses

e_c	1/20	1/35	1/50
$\sigma_{x,max}^{(uf)(AN)}$ [MPa]	78.12	89.69	98.33
$\sigma_{x,max}^{(uf)(FEM)}$ [MPa]	77.51	87.44	95.14
Δ	0.781	2.509	3.244

An exemplary distribution of normal stresses in the end part of the beam is presented in Fig. 6.

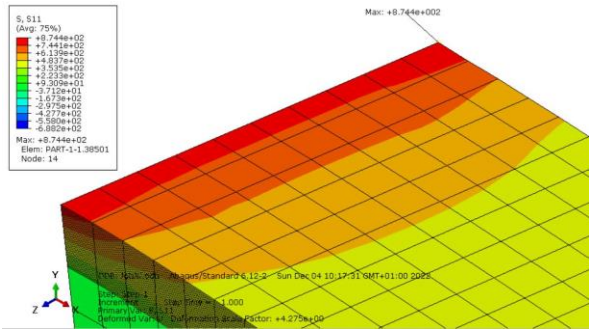

Fig. 6. Distribution of normal stresses in the end part of the beam

The comparison of the results obtained analytically and numerically shows that the differences in the maximum deflection values are less than 1%. In turn, the differences between normal stresses obtained from analytical and numerical research are below 3.5%.

4. Conclusions

In this article the bending of the sandwich beam with clamped ends was considered. The analytical model of this beam was developed according to the "broken-line" theory. Particular attention was paid to the shear effect and its influence on the value of deflection and normal stresses in the end parts of the beam.

The analytical research have shown that the shear effect has a significant influence on deflection and normal stresses. It can be easily noticed taking into account C_{se} values. The values of this coefficient range from 0.2 to 0.5 (Table 1) and from 0.6 even to 0.9 (Table 2). This means that the share of the shear effect in deflection is up to 50%, and in normal stresses up to 90%.

For comparision, an analogous numerical model was developed. Abaqus software was used both for modeling and calculating. Differences in deflection values obtained from analytical and numerical research were below 1%. In turn, the values of normal stresses in end part of the beam differ by a maximum of 3.5%.

The considered beam can be used in the construction of rail vehicles as a structural element of the body, e.g. the floor of a rail vehicle.

Bibliography

[1] Birman V, Kardomateas GA. Review of current trends in research and applications of sandwich structures. Compos Part B-Eng. 2018;(142):221-240. https://doi.org/10.1016/j.compositesb.2018.01.027

[2] Carrera E, Brischetto S. A survey with numerical assessment of classical and refined theories for the analysis of sandwich plates. Appl Mech Reviews. 2009;(62):01080-1-17. https://doi.org/10.1115/1.3013824

[3] Hao W, Xie J, Wang F. Theoretical prediction for large deflection with local indentation of sandwich beam under quasi-static lateral loading. Compos Struct. 2018;(192):206-216. https://doi.org/10.1016/j.compstruct.2018.02.097

[4] Icardi U. Applications of Zig-Zag theories to sandwich beams. Mech Adv Mater Struc. 2003;10(1):77-97. https://doi.org/10.1080/15376490306737

[5] Kozak J. Stalowe panele sandwicz w konstrukcjach okrętowych. Wyd. Politechniki Gdańskiej, 2018. Gdańsk. ISBN 978-83-7348-742-0.

[6] Kustosz J, Magnucki K, Goliwąs D. Bending of a stepped sandwich beam: the shear effect. Engineering Engineering Transactions. 2022;70(4):373-390. https://doi.org/10.24423/EngTrans.2238.20221125

[7] Magnucki K. Bending of symmetrically sandwich beams and I-beams – analytical study. International Journal of Mechanical Sciences. 2019;(150):411-419. https://doi.org/10.1016/j.ijmecsci.2018.10.020

[8] Magnucki K, Alsdorf D, Lewiński J, Kowalski M, Richter A, Zbierski A. Analytical, FEM-numerical and experimental studies of bending of a sandwich plate-strip with metal foam core. Rail Vehicles/ Pojazdy Szynowe. 2020;(3):1-19. https://doi.org/10.53502/RAIL-138552

[9] Magnucki K, Magnucka-Blandzi E, Wittenbeck L. Three models of a sandwich beam: Bending, buckling and free vibration. Engineering Transactions. 2022; 70(2):97-122. https://doi.org/10.24423/EngTrans.1416.20220331

[10] Sayyad AS, Ghugal YM. Modeling and analysis of functionally graded sandwich beams: a review. Mechanics of Advanced Materials and Structures. 2019;26(21):1776-1795. https://doi.org/10.1080/15376494.2018.1447178